www.ietdl.org

Published in IET Renewable Power Generation
Received on 21st September 2012
Revised on 17th February 2013
Accepted on 2nd March 2013
doi: 10.1049/iet-rpg.2012.0255

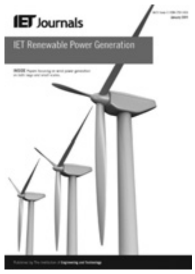

ISSN 1752-1416

Impact of wind power plant reactive current injection during asymmetrical grid faults

Ömer Göksu[1], Remus Teodorescu[1], Claus Leth Bak[1], Florin Iov[2,1], Philip Carne Kjær[2]

[1]*Department of Energy Technology, Aalborg University, Aalborg 9220, Denmark*
[2]*Vestas Wind Systems A/S, Århus 8200, Denmark*
E-mail: omg@et.aau.dk

Abstract: As more renewable energy sources, especially more wind turbines (WTs) are installed in the power system; grid codes for wind power integration are being generated to sustain stable power system operation with non-synchronous generation. Common to most of the grid codes, wind power plants (WPPs) are requested to stay connected and inject positive-sequence reactive current in order to boost positive-sequence grid voltage during short-circuit grid faults, irrespective of the fault type; symmetrical or asymmetrical. However, as shown in this study, when WPPs inject pure positive-sequence reactive current in case of asymmetrical faults, as a conventional method (CM) in accordance with the grid code requirement, positive-sequence grid voltage is boosted, but also higher negative sequence voltage in the grid and higher overvoltages at the non-faulty phases occur. In this study, an alternative injection method, where WTs are injecting both positive and negative sequence currents during asymmetrical faults, providing improved grid support, is given and compared with the CM. In addition, effect of coupling between positive, negative and zero sequences when WPPs are injecting currents during asymmetrical faults, is investigated, which was not considered in the wind power impact studies before.

1 Introduction

An important issue for modern power system is the increase of renewable energy units in the system, especially the wind energy, which has the highest share today [1]. As the installation of wind turbines (WT) is increasing, their impact on the power system stability is more considered, and extent of grid code requirements for wind power set by different transmission system operators are increasing [2]. It can be considered that the WTs are required to act in close manner to the synchronous generators of the conventional power plants (CPP). As a common requirement in most of the grid codes of certain countries, WTs are expected to stay connected and to support the positive-sequence grid voltage with positive-sequence reactive currents during short-circuit grid faults, for both symmetrical and asymmetrical faults. For instance, in the German grid code there is a reactive current requirement from WTs proportional to the drop of positive-sequence voltage, as shown in Fig. 1*a* [3]. In [4–7], benefits obtained with the reactive current injection from WTs are thoroughly analysed in terms of power system stability. It is shown in these studies that rotor angle stability of conventional synchronous generators connected nearby the wind power plant (WPP) is considerably improved if the WPP is supporting the grid with reactive current injection during faults.

As well-known from power system analysis, faults can be classified mainly as symmetrical and asymmetrical. During both symmetrical and asymmetrical faults positive-sequence voltage drops down, whereas during asymmetrical faults also negative and zero-sequence voltages and currents arise in the grid. Asymmetrical faults in overhead lines (OHLs) of the transmission grid are occurring more frequently as single line-to-ground faults with 70%, line-to-line faults with 15%, double line-to-ground faults with 10%, than symmetrical faults with 5% occurrences [8]. However, grid codes are prepared to target only positive-sequence voltage boost, which can be considered as a proportional voltage control in positive-sequence. There are few requirements prepared specifically for asymmetrical faults or negative sequence current injection. For instance, in German grid code [3] the maximum reactive current requirement, which is 1 pu for symmetrical faults, is requested as a lower value of 0.4 pu for asymmetrical faults; and informative statement is given about existence of negative sequence current flow in German and Spanish grid codes. In latest network code of the ENTSO-E, negative sequence current injection is stated to be defined by agreements between system and plant operators [9].

Negative sequence voltages in the grid are tried to be kept small mainly for continuous and also for short-term operation, since negative sequence current flow has detrimental effects as excessive heat, physical wearing and power oscillations [10–13]. Also during asymmetrical faults, phase-to-ground voltages in non-faulty phases rises over rated values, that is, phase overvoltages occur. Neutral grounding of the power system is designed to keep zero-sequence impedances in accordance with the target of avoiding high-phase overvoltages but also avoiding very high-fault currents during asymmetrical faults [10].

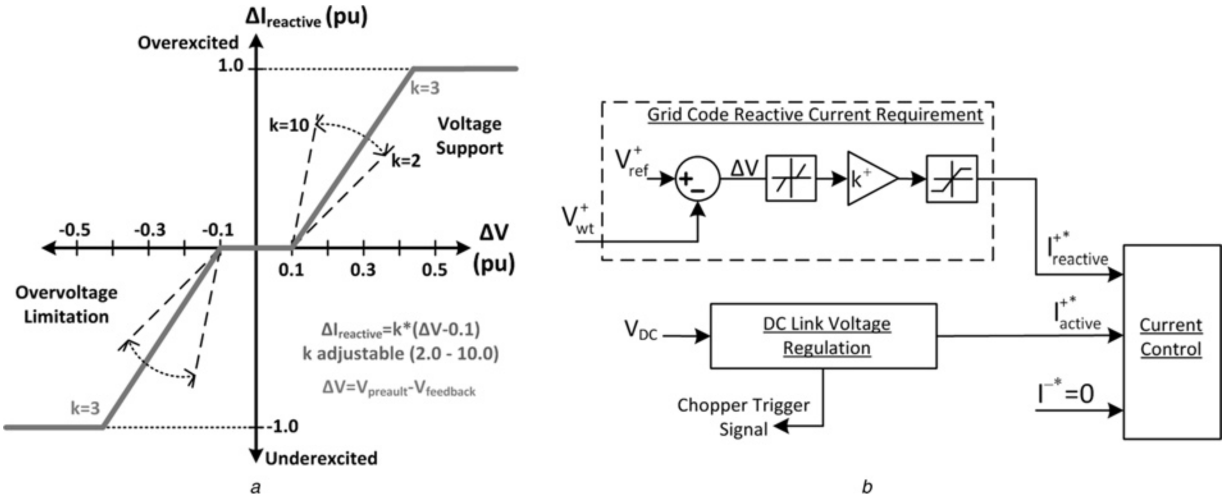

Fig. 1 *Grid code positive sequence reactive current requirement and WT control structure*

a Reactive current requirement of German grid code [3]
b Conventional Method

In conjunction with the strict grid code requirements, advanced solutions for the WTs and WPPs are developed by the manufacturers, which can comply with the demanding grid codes [14, 15]. The modern variable speed WTs based on doubly-fed induction generators (DFIG), and full converter WT (FCWTs) have the capability to behave as controlled current sources controlling their grid currents independently as active and reactive components for both positive and negative sequences [14–16]. In Fig. 1*b*, the conventional method (CM) that complies with the positive-sequence reactive current injection requirement of the grid code is given. The CM shown in Fig. 1*b* is realising the grid code positive-sequence voltage control requirement via generating positive-sequence reactive current reference proportional to the positive-sequence voltage drop; and the remaining current capacity of the WT is utilised as positive-sequence active current. The negative sequence current reference is kept as zero, which provides pure positive-sequence (symmetrical) current injection. The voltage reference, V_{ref}^{+}, can be taken as the rated value, that is, 1 pu, or the prefault voltage value. A deadband can be applied to voltage error, which is defined as 0.1 pu in certain grid codes [3]. The proportional voltage control gain, k^{+}, is adjusted based on the characteristics of the power system, and specified to be between 2 and 10 [3].

The structure of the FCWT, which is the WT type used in this study, is shown in Fig. 2. The generator side converter, the generator itself and the rotor aerodynamics of the FCWT are represented as a constant power source since these parts have low bandwidth compared with the short duration of the faults [17]; and the grid side converter, dc-link and the chopper resistance are modelled since these parts are the main components functioning during a fault [18]. T_{chop}^{*} is the triggering signal for the chopper resistance switch, which is used to dissipate any excess power flowing from the generator side to avoid over voltages at the dc-link during faults [17]. The current control block of the FCWT performs current regulation [14], keeping the phase current magnitudes within defined limits while giving priority to reactive current reference, and generates T_{ABC}^{*} modulation signals for the grid side converter. The current controller is based on a stationary frame proportional resonant (PR) current regulator [19], which works in coordination with a grid synchronisation algorithm, a dual second order generalised integrator-based frequency-locked loop (DSOGI-FLL) [20]. The DSOGI-FLL extracts and provides the positive and negative sequence components of the grid voltage, which are used to obtain active and reactive current references in positive and negative sequences in alpha-beta frames, and also to detect positive-sequence voltage drop and negative sequence voltage magnitude in the grid. Output phase voltages and currents are kept within ratings (e.g. 1 pu) via continuously calculating and scaling down the current and voltage references in case any phase exceeds the maximum. As per grid code requirement, priority is given to reactive current during faults, which in turn means reduced or zero active current injection.

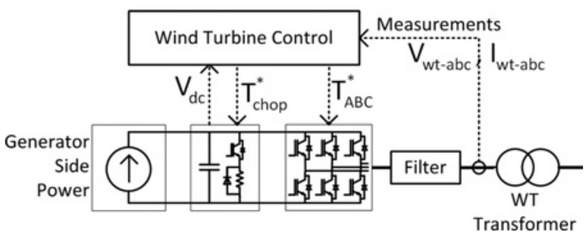

Fig. 2 *FCWT under study*

Independent control of active and reactive currents in positive and negative sequences under unbalanced grid conditions is proven capability for grid connected converters [14], such as full-converter type WTs as used in this paper. In the literature, this current control capability in positive and negative sequences is utilised for various purposes; for example, to mitigate twice fundamental frequency oscillations arising in the dc-link during asymmetrical faults [21–24], and to mitigate grid voltage unbalance [25–27]. However, in these studies, the problem is approached from power electronics control point of view at the WT level; whereas in this paper, the problem is approached from power systems point of view considering the sequence networks, neutral grounding, phase overvoltages and the coupling between sequences. Different from the state-of-the-art studies, in this paper the impact of WPP current injection on the power system is analysed.

Adverse effects observed with the CM are shown; and target of improved grid support at power system level is performed in this paper. The controlled current injection capability of the WT is utilised, whereas the issues at the WT level, such as dc-link voltage oscillations, are not targeted.

As will be shown in following parts, when the CM of injecting pure positive-sequence current is employed in case of asymmetrical grid faults, all three phases of the grid voltage, including the non-faulty phase(s) are boosted. Since negative sequence current injection of WPP is kept as zero, which means that WPP behaves as open circuit in negative sequence, negative sequence voltage is not attenuated and propagates towards the WPP. In addition, because of coupling between positive, negative- and zero-sequence networks during asymmetrical faults, which will be shown in following parts, negative and zero-sequence voltages are additionally boosted at the fault point. As a result of above mentioned issues, higher negative sequence voltage and higher phase overvoltages can be observed towards WPP, because of the support of WPP utilising CM.

In this paper; first a comparison is done in Section 2 between fault responses of a CPP, which is based on a conventional synchronous generator and a WPP, which is injecting pure positive-sequence current. For the first time in this paper, the above-mentioned coupling between positive, negative and zero-sequence networks is investigated by utilising equivalent circuits of asymmetrical faults in Section 3. In Section 4, the alternative control method dual-sequence (DS), which is providing improved grid support via realising voltage support during asymmetrical faults in both positive and negative sequences, is given. In addition, existing methods injecting in both positive and negative sequences are reviewed in that section. At the end, impact of reactive current injection by means of described control methods are compared with time-domain simulations.

2 Comparison of a CPP and a WPP

To show power system impact of WPPs, which are injecting pure positive-sequence currents in accordance with the grid code requirement; two cases are compared in Fig. 3. In the first case, response of a CPP based on a synchronous generator to a single line-to-ground fault is shown, whereas in the second case CPP is supplanted by a WPP, which is injecting pure positive-sequence reactive current. The voltage magnitudes and phase angles are values at the steady-state period of the fault obtained from time-domain simulations using Matlab Simulink SimPowerSystems toolbox. In both cases power plants are connected radially to the main grid via 50 km long OHLs, which are modelled with their PI equivalents. Before the fault power plants are injecting 20% active power and the point of common coupling (PCC) voltage is regulated to 1 pu in both cases. Grid is represented with its Thevenin's equivalent. A single line-to-ground fault occurs at phase 'a', at the point where the OHL is connected to the main grid. The details of the main grid, OHL, CPP and WPP are given in the Appendix.

In zero sequence, which is not shown in Fig. 3 for clarity, both CPP and WPP give the same response since they both employ dYN transformers, which are grounding the neutral of the grid side, and also isolating the zero-sequence networks of power plant from the grid side [28]. Hence zero-sequence currents flow, and zero-sequence voltage is attenuated towards the power plants in both cases. As observed from Fig. 3, in positive-sequence both power plants are boosting the positive-sequence voltage by means of supplying fault currents. As expected, in the first case with CPP in Fig. 3, voltages at the faulted bus and the PCC bus are higher compared with the WPP case, since CPPs are able to inject higher current during faults thanks to the capability of conventional synchronous generators. As observed in Fig. 3, the CPP with high current capability can boost the positive-sequence voltage as 9% from 0.77 to 0.86 pu as more than the WPP, which boosts as 5% from 0.76 to 0.81 pu.

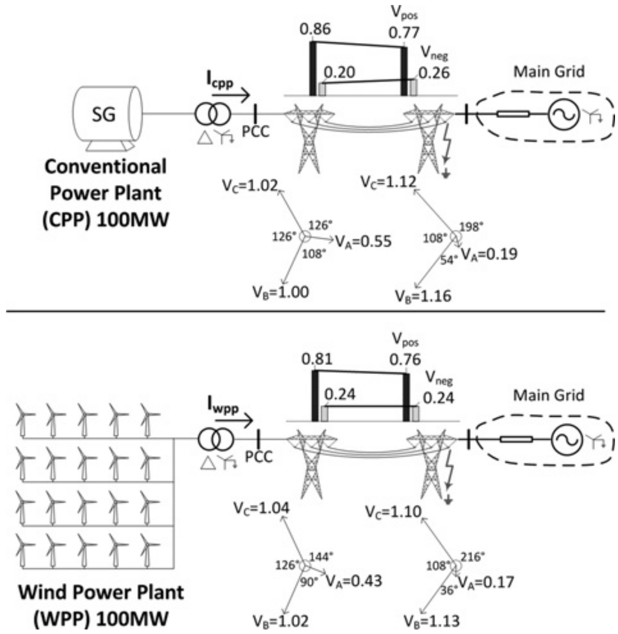

Fig. 3 *Comparison of a CPP; and a WPP injecting pure positive-sequence currents (CM)*

In negative sequence, CPP behaves as impedance and allows current flow, which attenuates the negative sequence voltage towards the CPP from 0.26 to 0.20 pu. Hence, phase voltages become both boosted and balanced towards 1 pu at the PCC of the CPP, such that the faulted phase 'a' is boosted from 0.19 to 0.55 pu and overvoltages at the non-faulty phases are attenuated close to 1 pu. However, since the WPP is injecting pure positive-sequence current, which in turn means not allowing flow of WPP negative sequence currents, WPP behaves as open circuit in negative sequence. Hence, as seen from Fig. 3, when CM is employed by the WPP, negative sequence voltage is not attenuated and propagates as 0.24 pu towards the PCC of the WPP. because of this response of WPP, phase voltages are not balanced effectively towards the WPP and 1.04 pu phase 'c' voltage exists at the PCC. It is important to note that phase overvoltages might not propagate towards WTs as same as PCC, since zero-sequence voltage does not propagate beyond the WPP transformer because of the use of dYN transformers.

3 Understanding of coupling phenomenon during asymmetrical faults

As well-known from power system fault analysis, positive, negative and zero-sequence networks are interconnected at the faulted point through the fault impedance [10, 29].

doi: 10.1049/iet-rpg.2012.0255

Hence, sequence voltages are coupled at the faulted bus. Owing to this coupling, an action in one of the sequences has effects also on the other sequences. It will be shown here and also in the following section with simulations that when a WPP boosts positive-sequence voltage via injecting pure positive-sequence currents, negative and zero-sequence voltages are also boosted at the faulted point, compared with the case that the WPP is not injecting any current. Amount of coupled boost in negative and zero sequences depend primarily on how much the voltage at the faulted point can be altered by the WPP, and also the fault type and fault impedance. Transfer impedance between the WPP and the faulted point defines how much the WPP can alter the voltage at the faulted bus; and the transfer impedance depends on the grid characteristics and fault location. It can be said that for weak grids (with high grid impedance) and/or for faults occurring near to WPP, coupling is more observed, since WPP can alter the bus voltage more for weak grids, than for a strong grid [30].

Coupling can be better understood when sequence voltages at the faulted point is compared for two cases as; with and without current injection from WPP during the fault. Equivalent circuits are utilised to show effect of coupling during a double-line-to-ground fault as given in Fig. 4 [8, 10, 29]. Impact of positive-sequence voltage boost obtained by the WPP current injection is superimposed to the positive-sequence equivalent voltage, and resulting impact on the negative and zero sequences are simply calculated. It is known from power system fault analysis that the equivalent voltage source V_{th}^{+} is the prefault voltage at the fault point, which depends on the power flow before the fault and usually kept at rated (1 pu) value via voltage control action of power plants. However, positive-sequence reactive current injection by WPPs during fault can be considered as additional reactive power support which was not given before the fault, and which increases the voltage at the faulted point. Boost obtained by the WPP current injection on the faulted point, $V_{\Delta\mathrm{wpp}}^{+}$, can be calculated as (1) by using the positive-sequence transfer impedance Z_{fw}^{+}, from the WPP current injection bus to the faulted point and the WPP current I_{w}^{+} , which is the WPP current phasor.

$$V_{\Delta\mathrm{wpp}}^{+} = Z_{\mathrm{fw}}^{+} I_{\mathrm{w}}^{+} \tag{1}$$

It should be noted that (1) is representing the voltage boost at the faulted bus obtained by the WPP current injection, which is basically originating from node voltage equation of the network. In the previous section and in the following sections, WPP is modelled in time-domain as a three-phase voltage source converter including its current controller with details given in the introduction. Assuming the positive and negative sequence impedances as equal [10, 29], via simply voltage division, remaining voltages for a double line-to-ground fault and effect of WPP support can be obtained as in (2) to (4). It is important to note that the voltage boost by WPP, $V_{\Delta\mathrm{wpp}}^{+}$, and the impedance Z_{ff}^{+}, Z_{ff}^{-} and Z_{ff}^{0}, are complex quantities. Based on the equations derived below approximate calculations can be done for sequence voltages, which will be used for understanding of coupling action. Detailed and precise analysis requires time-domain simulations, which will be given in the following parts.

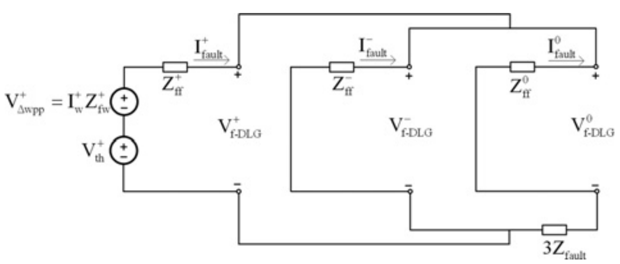

Fig. 4 *Equivalent circuits during double line-to-ground fault*

$$\begin{aligned} V_{\mathrm{f-DLG}}^{+} &= \left(V_{\mathrm{th}}^{+} + I_{\mathrm{w}}^{+} Z_{\mathrm{fw}}^{+}\right)\left(\frac{Z_{\mathrm{ff}}^{-}//(Z_{\mathrm{ff}}^{0}+3Z_{\mathrm{f}})}{Z_{\mathrm{ff}}^{+}+Z_{\mathrm{ff}}^{-}//(Z_{\mathrm{ff}}^{0}+3Z_{\mathrm{f}})}\right) \\ &= \left(Z_{\mathrm{th}}^{+} + V_{\Delta\mathrm{wpp}}^{+}\right)\left(\frac{Z_{\mathrm{ff}}^{0}+3Z_{\mathrm{f}}}{Z_{\mathrm{ff}}^{-}+2Z_{\mathrm{ff}}^{0}+6Z_{\mathrm{f}}}\right) \end{aligned} \tag{2}$$

$$\begin{aligned} V_{\mathrm{f-DLG}}^{-} &= \left(V_{\mathrm{th}}^{+} + I_{\mathrm{w}}^{+} Z_{\mathrm{fw}}^{+}\right)\left(\frac{Z_{\mathrm{ff}}^{-}//(Z_{\mathrm{ff}}^{0}+3Z_{\mathrm{f}})}{Z_{\mathrm{ff}}^{+}+Z_{\mathrm{ff}}^{-}//(Z_{\mathrm{ff}}^{0}+3Z_{\mathrm{f}})}\right) \\ &= \left(V_{\mathrm{th}}^{+} + V_{\Delta\mathrm{wpp}}^{+}\right)\left(\frac{Z_{\mathrm{ff}}^{0}+3Z_{\mathrm{f}}}{Z_{\mathrm{ff}}^{-}+2Z_{\mathrm{ff}}^{0}+6Z_{\mathrm{f}}}\right) = V_{\mathrm{f-DLG}}^{+} \end{aligned} \tag{3}$$

$$\begin{aligned} V_{\mathrm{f-DLG}}^{0} &= \left(\frac{Z_{\mathrm{ff}}^{0}}{Z_{\mathrm{ff}}^{0}+3Z_{\mathrm{f}}}\right) V_{\mathrm{f-DLG}}^{+} \\ &= \left(V_{\mathrm{th}}^{+} + V_{\Delta\mathrm{wpp}}^{+}\right)\left(\frac{Z_{\mathrm{ff}}^{0}}{Z_{\mathrm{ff}}^{-}+2Z_{\mathrm{ff}}^{0}+6Z_{\mathrm{f}}}\right) \simeq V_{\mathrm{f-DLG}}^{+} \end{aligned} \tag{4}$$

As observed in Fig. 4 and in (2) to (4), for a double line-to-ground fault, the positive and negative sequence voltages at the faulted point are inevitably equal. Hence, if the positive-sequence voltage is boosted by the WPP at the faulted point, the negative sequence voltage is also inevitably boosted to the same value because of coupling. When the fault impedance (e.g. 0.02 pu), which is small compared with positive-sequence impedance (e.g. 0.2 pu), is neglected, zero-sequence voltage is also equal to the positive-sequence voltage, thus the zero-sequence voltage is also boosted with almost the same amount. For instance, for a system with magnitude of Z_{fw} 0.2 pu, it can be said that 1 pu WPP reactive current injection would boost positive-sequence voltage approximately by 0.1 pu based on (2), but also the negative and zero-sequence voltages with the same amount as seen in (3) and (4).

Analysing the equivalent circuits for single-line-to-ground and line-to-line faults [8, 10, 29], which are not shown here because of space limitations, coupling between positive negative and zero-sequence voltages can be observed as similar to the double line-to-ground case shown here.

The coupling explored here has not been observed in previous wind power studies, since the asymmetrical faults have not been created as realistic events as short-circuits (solid or with a fault impedance) between phases and/or ground; instead unbalance was being created via modifying voltage sources, which represent grid voltage, in the simulation models. Hence, in previous studies, interconnection of positive negative and zero sequences did not exist and it was observed that when the positive-sequence voltage is boosted via injecting pure positive-sequence currents, negative sequence voltage remains unaffected. For instance in [25, 26], it is stated that the negative sequence voltage remains unaffected when pure positive-sequence current is injected, since the coupling phenomenon, which is studied here, has not been considered in the previous studies. However, as shown here, it is important to conduct real faults for asymmetrical fault studies in order to observe interconnection between sequences, especially for high wind power penetration cases.

It is important to note that coupling also exists from negative sequence to positive and zero sequences, such that when negative sequence voltage is attenuated by WPPs, positive-sequence voltage is also attenuated because of coupling. Hence at the faulted bus it becomes as a trade-off between boosting positive-sequence voltage and balancing the phase voltages.

4 Dual-sequence voltage support

The response of WPPs during asymmetrical faults have been studied in the literature [21–27], and several control methods injecting negative sequence current have been proposed; for example, to mitigate power and dc-link voltage oscillations from the WT [21–24], for example, to balance the grid voltage by reducing the negative sequence voltage [25–27]. However, these methods mainly deal with issues related to WTs themselves or include negative sequence voltage attenuation at the WT level, whereas in this paper the situation is handled considering the grid side impact of the WPP current injection during asymmetrical faults. Impact of WPP's pure positive-sequence current injection during asymmetrical faults is given in the previous sections. It is shown that, a WPP, employing CM, is causing high negative sequence voltage and high-phase overvoltages since WPP is acting as open circuit in negative sequence. Alternative to the CM, which is injecting pure positive-sequence reactive (capacitive/overexcited) currents by WPPs, the concept of DS voltage support is represented here. DS is based on injecting both positive-sequence reactive (capacitive/overexcited) currents boosting the positive-sequence voltage and negative sequence reactive (inductive/underexcited) currents reducing the negative sequence voltage towards zero, as given in Fig. 5. As explained in the introduction section, the DSOGI-FLL [20] grid synchronisation algorithm is utilised to extract the positive and negative sequence voltages and currents from the measured unbalanced three-phase variables and the PR current regulator is controlling the current independently as

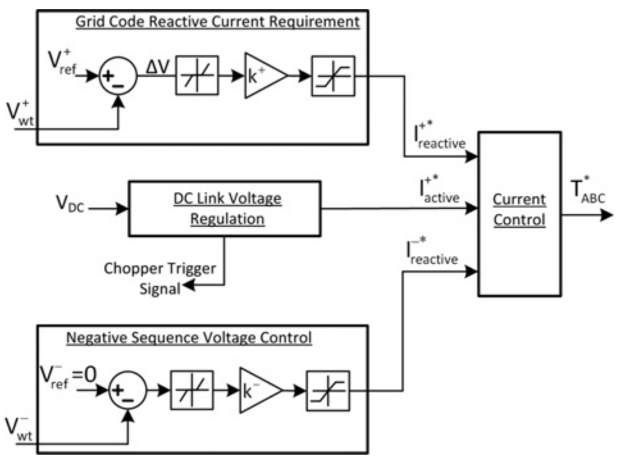

Fig. 5 *DS voltage support method*

active and reactive in positive and negative sequences [19]. The DS method is based on this injection capability of WTs.

In contrast to the CM, where all phases, hence including the non-faulty phases are supported, the DS method distributes the support such that only faulted phases are supported, and non-faulty phases are not supported unnecessarily. Hence, high-phase overvoltages in the non-faulty phases are mitigated, and support is shared as between positive-sequence voltage boost and negative sequence voltage reduction. The DS method is shown in Fig. 5, where the main additional function of DS method is the negative sequence voltage control in parallel to positive-sequence voltage control. Hence in DS method, there is also negative sequence proportional voltage control gain k^-, in addition to the positive-sequence proportional voltage control gain, k^+, which was shown in conventional control method in Fig. 1*b*. These parameters can simply be tuned as having identical values, as is done in this study, whereas alternative tuning methods can be accomplished for setting different priorities between boosting positive and reducing negative sequence voltages. With the use of DS method, WPP behaves as impedance in negative sequence attenuating the negative sequence voltage towards the WPP, similar to a CPP. Performance of the DS method is compared with two other methods in the next section with simulations.

5 Simulation results

The performance of the DS method, which is injecting both positive and negative sequence currents, is compared against the CM in this section. In order to see the bus voltages during faults without support of the WPP, a third injection method of no support (NS), where WPP is keeping its currents as zero, is also implemented as a reference. Three injection methods, namely NS, CM and DS are simulated utilising Matlab Simulink SimPowerSystems toolbox. In the simulations WPP with 100 MW rating is aggregated as single WT [31]. WT converter is modelled with average voltage sources, neglecting switching behaviour [18], employing DSOGI-FLL grid synchronisation and a stationary frame PR active/reactive current controller for both positive/negative sequences [14, 19, 20]. DC-link is assumed to be regulated by the WT machine side also utilising chopper resistance [17]. The system used in the simulations, and its equivalent circuits for sequences are shown in Fig. 6. The negative sequence network is the same as the positive-sequence network except with zero grid voltage. The grid is modelled with its Thevenin equivalent and the WPP is connected to the grid via 50 km long OHL. The OHL and collector network equivalent are modelled as PI models. In the WPP d5YN and ynD5 type transformers are utilised as WPP main transformer and WT transformer, respectively. The collector network's neutral is grounded via a grounding zigzag transformer. Details of the grid, transformers, OHL, WPP and CPP are given in Appendix section.

In the WT, deadband in the voltage control algorithms are kept as zero, that is, not applied. Proportional voltage control constant, k^+, for the CM (control structure given in Fig. 1*b*) case is selected as 5, and the two proportional constants, k^+ and k^- for DS (control structure given in Fig. 5) case are both kept identical as 2.5. The maximum current that can be injected by the WPP is kept as 1 pu. In order to show

doi: 10.1049/iet-rpg.2012.0255

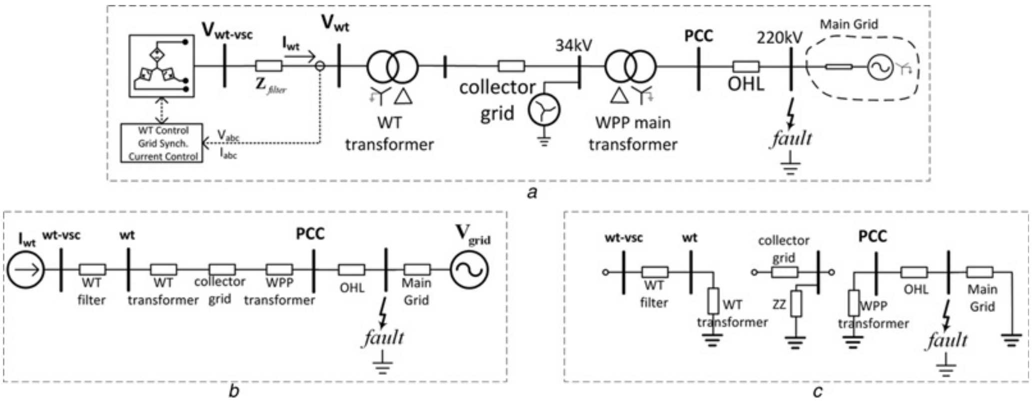

Fig. 6 *System used in the simulations, and its equivalent circuits for sequences*

a Single-line diagram of the simulated fault case
b Positive- and negative-sequence networks
c Zero-sequence network

impact of WPP reactive current injection on grid voltages clearly, only reactive currents are injected during the fault and active current is kept as zero. As explained in the introduction part, active current is injected when there is remaining capacity since the priority is given to reactive current as per the grid code requirement.

Time-domain response for a single-line-to-ground fault is shown in Fig. 7, where the fault is created at phase 'a'. In order to save space, all three control algorithms are executed during the fault, keeping the fault duration intentionally long as 300 ms. Fault is created at $t = 1.1$ s, which is removed at $t = 1.4$. Before and after the fault, the WPP is injecting 20% active power and 0.2 pu balanced phase currents are seen in Fig. 7*a*. For the first 100 ms of the fault, WPP currents are kept zero, that is, NS is applied, in order to observe the case without the WPP support. Since the active power component of the current is kept zero during the fault in order to show the reactive current components clearly, the rms current values shown in Fig. 7*b* are pure reactive components for both positive and negative sequences. At $t = 1.2$, CM is activated and pure positive-sequence currents are injected as a positive-sequence proportional voltage control. At $t = 1.3$, the DS method is activated and both positive and negative sequence voltage control are realised via injecting both positive and negative sequence currents. In Fig. 7*d*, V_F represents the voltage at the faulted point.

As seen in Fig. 7*c*, at the faulted bus the healthy phase voltages, which are 1.08 pu without WPP support, rise up to 1.13 pu, when CM is employed. Similarly at PCC, healthy phases are unnecessarily boosted from 0.95 to 1.04 pu value when CM is employed, as shown in Fig. 7*e*. However, with the use of DS method, at the PCC bus positive-sequence voltage is boosted to 0.78 pu, negative sequence voltage is attenuated to 0.23 pu and phase overvoltage is mitigated.

It is important to note in Fig. 7*d* that even though the zero-sequence networks of grid and WPP are isolated with the use of dYN transformer, the zero-sequence voltage at the faulted bus is still increased with use of CM, when compared with NS because of coupling between sequences. It rises inevitably also for DS, but nevertheless negative sequence voltage is attenuated with DS, providing balanced voltages.

Since the focus is only on the steady-state period of the faulted duration and in order to save space, for double-line-to-ground and line-to-line faults, time-domain results are given in Tables 1 and 2, showing values for steady-state period of each algorithm. As observed in results of double line-to-ground fault, given in Table 1, at the faulted bus, with CM all the phase voltages are boosted, which means the non-faulty phase 'a' is boosted unnecessarily by 10% from 1.11 to 1.21 pu and the positive-sequence voltage, but also the negative sequence voltage because of the coupling, are both boosted 4%, from 0.39 to 0.43 pu. Hence high overvoltages are observed at the faulted bus and the PCC bus. However, DS method is boosting the positive-sequence voltage from 0.39 to 0.47 pu while attenuating the negative sequence voltage from 0.39 to 0.35 pu at the PCC bus, avoiding unnecessary support to non-faulty phase 'a' via boosting only the faulted buses, 'b' and 'c', whereas non-faulty phase 'a' is slightly boosted to 0.91 pu. It should be noted that DS method is boosting and balancing at the PCC compromising high boost obtained by CM, which is from 0.39 to 0.54 pu.

Results for a line-to-line fault are given in Table 2, where it is seen that with the use of CM both the positive and negative sequence voltages are boosted with the same amount of 0.03 pu at the faulted bus because of the coupling, where the non-faulty phase 'a' is boosted unnecessarily from 1 to 1.06 pu; and at the PCC bus the non-faulty phase 'a' is boosted from 1.01 to 1.12 pu. Owing to the coupling between positive and negative sequences at the faulted bus the DS method is compromising boost of positive-sequence voltage while avoiding the boost of the negative sequence voltage. With the balancing effect of the DS method, at the PCC bus positive-sequence voltage is boosted and negative sequence voltage is attenuated such that the support is distributed and non-faulted phases are not boosted.

As seen in Fig. 7, the dc-link voltage oscillation is decreasing from 0.3 to 0.12 pu when compared with the CM case for single line-to-ground fault, and from 0.6 to 0.04 pu for line-to-line fault as given in Table 2. However, as seen in Table 1, for double-line-to-ground fault the dc-link voltage oscillation is increasing from 0.2 to 0.34 pu, with the use of DS method. It should be noted that in this paper impact of WPP reactive current injection on the power system is analysed and improved grid support in the sense of mitigation of phase overvoltages and balance of grid voltages; however, impact on the WT level, such as dc-link voltage oscillations, is not targeted to be mitigated. However, the proven method of dc-link voltage oscillations

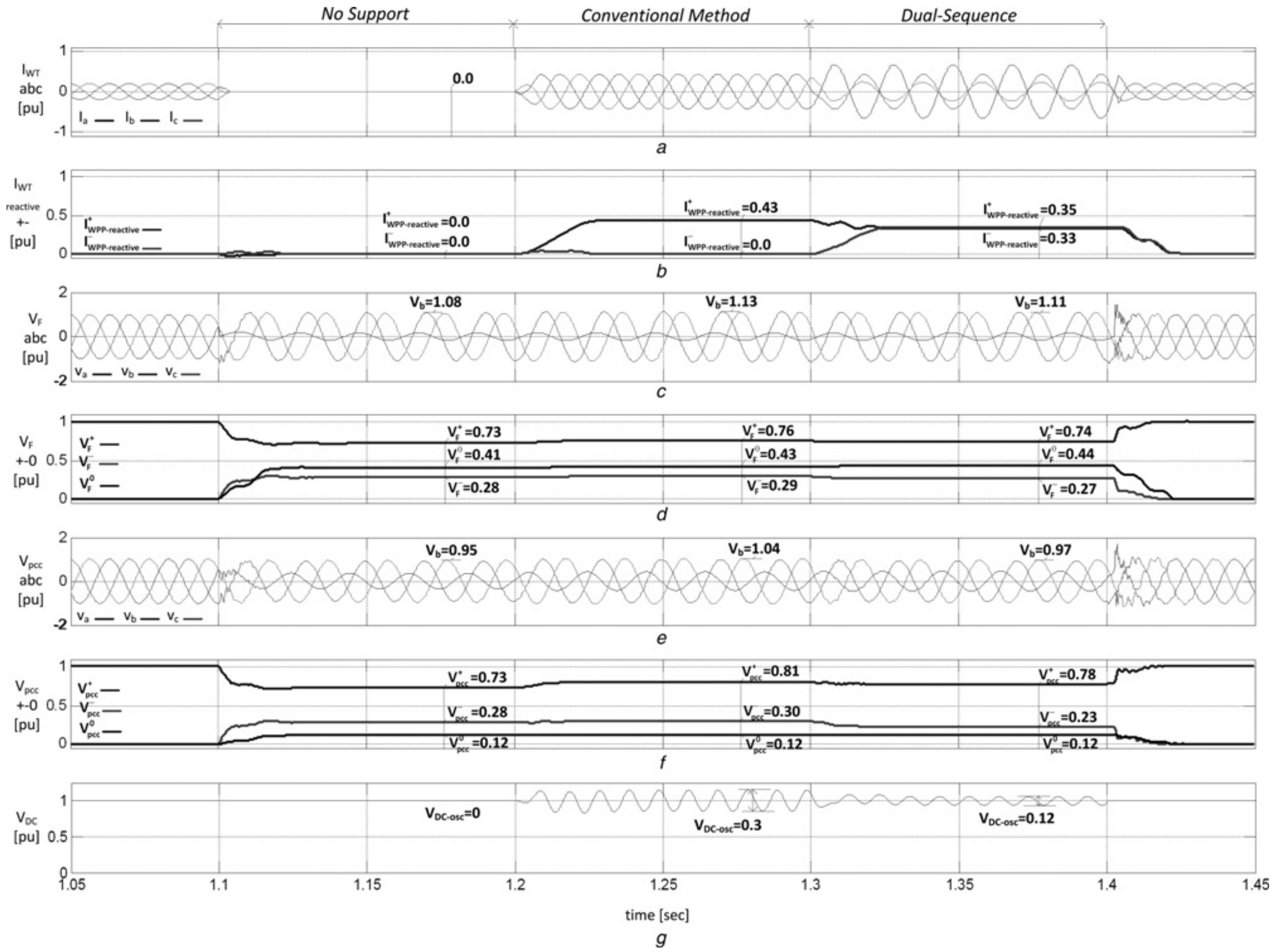

Fig. 7 *Simulation results for a single-line-to-ground fault*

a WT phase currents
b WT positive- and negative-sequence rms current values
c Faulted point phase voltages
d Faulted point positive-, negative-, and zero-sequence rms voltage values
e PCC phase voltages
f PCC positive-, negative-, and zero-sequence rms voltage values
g Calculated DC link voltage

Table 1 Simulation results for a double-line-to-ground fault [pu]

		NS	CM	DS
I_{wt}	Pos.	0	1.00	0.60
	Neg.	0	0	– 0.40
	a	0	1.00	0.21
	b	0	1.00	0.85
	c	0	1.00	0.89
V_F	Pos.	0.39	0.43	0.40
	Neg.	0.39	0.43	0.40
	Zero	0.35	0.38	0.35
	a	1.11	1.21	1.13
	b	0.14	0.16	0.14
	c	0.14	0.16	0.14
V_{pcc}	Pos.	0.39	0.54	0.47
	Neg.	0.39	0.43	0.35
	Zero	0.10	0.11	0.10
	a	0.87	1.06	0.91
	b	0.31	0.42	0.35
	c	0.31	0.40	0.34
$V_{DC\text{-}osc}$	—	0.00	0.20	0.34

Table 2 Simulation results for a line-to-line fault (pu)

		NS	CM	DS
I_{wt}	Pos.	0	0.53	0.49
	Neg.	0	0.0	– 0.51
	a	0	0.53	0.12
	b	0	0.53	0.80
	c	0	0.53	0.92
V_F	Pos.	0.51	0.54	0.51
	Neg.	0.49	0.52	0.49
	Zero	0.00	0.00	0.00
	a	1.00	1.06	1.00
	b	0.59	0.62	0.59
	c	0.42	0.44	0.41
V_{pcc}	Pos.	0.51	0.60	0.57
	Neg.	0.50	0.52	0.44
	Zero	0.00	0.00	0.00
	a	1.01	1.12	1.01
	b	0.59	0.67	0.62
	c	0.42	0.46	0.41
$V_{DC\text{-}osc}$	—	0.00	0.60	0.04

doi: 10.1049/iet-rpg.2012.0255

[21–24] can be considered to be combined with the target of improved grid support. Effect of grid voltage phase jump during fault is not investigated in this paper. In [32], it is shown that the high bandwidth current control capability of FCWTs, which is utilised in this paper, provides robustness against phase jumps during transients of the faults. However, as investigated in [33], such phase jumps can cause detrimental effects as high rotor currents, torque oscillations in case of implementation to DFIG type WTs, which should be considered separately.

As seen from Fig. 7, Tables 1 and 2, with the use of DS method, peak values of WT phase currents are decreased, which also gives chance to additional utilisation of the WT for more currents to inject more reactive or active power during the fault.

In summary, when only positive-sequence reactive current is injected in the case of CM, non-faulty phases are also boosted unnecessarily, which causes severe increase in the phase-to-ground voltages of non-faulty phases. The DS method is shown to be able to mitigate adverse effects of the CM, effect of coupling on negative sequence voltage is successfully mitigated, negative sequence voltage is attenuated towards WPP, and high-phase overvoltages are avoided. As a drawback of DS method the grid voltages are both boosted and balanced for the expense of less amount of boost of positive-sequence voltage.

6 Conclusions

Impact of the WPP reactive current injection is analysed in this paper. A CM, which is injecting pure positive-sequence (symmetrical) currents in accordance with the grid code requirements, is implemented for a WPP, and response is compared with response of a CPP, which is based on synchronous generator. It is shown that, WPP with pure positive-sequence current injection is boosting all the phases, including the non-faulty phases and behaving as open circuit in negative sequence. Hence negative sequence voltage propagates towards the WPP, which causes higher negative sequence voltages. In addition, because of coupling between sequences, negative and zero-sequence voltages are also boosted at the faulted point. Owing to all abovementioned issues, higher phase overvoltages are observed, as reactive power is injected for healthy phases unnecessarily with pure positive-sequence reactive current injection.

An alternative to CM, the DS method, which is realising voltage control in both positive and negative sequences, is given and shown to solve adverse effects caused by CM. The DS method is boosting only the faulted phases and balancing the grid voltages. In other words, with the use of DS method WPP behaves as impedance in negative sequence during asymmetrical faults, similar to a CPP, boosting the positive-sequence voltage and attenuating the negative sequence voltage.

In addition, coupling between sequences is explored and effects are shown for the first time, which was not considered in the fault analysis studies with wind power before. Approach for fault modelling for asymmetrical fault studies is given in this manner, which should be considered especially for high wind penetration scenarios.

As a final comment, results provide insight for impact of positive and negative sequence current injection by WPPs on the grid, which can be used for assessment of negative sequence current injection requirements to be included in the future grid codes of countries with high renewables based generation.

7 Acknowledgments

This work was supported by Aalborg University-Vestas Wind Systems A/S partnership under Vestas Power Programme. Any opinions, findings and conclusions or recommendations expressed in this material are those of the authors and do not necessarily reflect those of Vestas Wind Systems A/S. Support from Pedro Rodriguez, from Department of Electrical Engineering, Technical University of Catalonia, Spain is highly appreciated and acknowledged.

8 References

1 BTM Consult ApS: 'International wind energy development, world market update', 2010
2 Tsili, M., Papathanassiou, S.: 'A review of grid code technical requirements for wind farms', *IET Renew. Power Gener.*, 2009, **3**, (3), pp. 308–332
3 Eon Netz GmbH: 'Grid code high and extra high voltage', online: http://www.eon-netz.com/, 2006
4 Ullah, N.R., Thiringer, T., Karlsson, D.: 'Voltage and transient stability support by wind farms complying with the E.ON Netz grid code', *IEEE Trans. Power Syst.*, 2007, **22**, (4), pp. 1647–1656
5 Kayikci, M., Milanovic, J.: 'Reactive power control strategies for DFIG based plants', *IEEE Trans. Energy Convers.*, 2007, **22**, (2), pp. 389–396
6 Engelhardt, S., Erlich, I., Feltes, C., Kretschmann, J., Shewarega, F.: 'Reactive power capability of wind turbines based on doubly fed induction generators', *IEEE Trans. Energy Convers.*, 2011, **26**, (1), pp. 364–372
7 Mohseni, M., Islam, S.: 'Transient control of DFIG-based wind power plant in compliance with the Australian grid code', *IEEE Trans Power Electr.*, 2012, **27**, (6), pp. 2813–2824
8 Anderson, P.M.: 'Analysis of faulted power systems' (IEEE Press, 1995, 1st edn.)
9 European network for transmission system operators for electricity: 'ENTSO-E network code for requirements for grid connection applicable to all generators', 26 June 2012
10 Das, J.C.: 'Power system analysis: short-circuit load flow and harmonics' (Marcel Dekker Press, 2002, 1st edn.)
11 Muljadi, E., Batan, T., Yildirim, D., Butterfield, C.P.: 'Understanding the unbalanced-voltage problem in wind turbine generation'. Proc. 34th IAS Annual Meeting, October 1999, vol. 2, pp. 1359–1365
12 Chen, K., Montgomery, L.W., Klempner, G. *et al.*: 'Comparing IEEE 50.13 and IEC 60034 standards for large cylindrical rotor synchronous machines'. Proc. IEEE Power and Energy Society General Meeting, July 2010, pp. 1–9
13 Gnacinski, P.: 'Windings temperature and loss of life of an induction machine under voltage unbalance combined with over- or undervoltages', *IEEE Trans. Energy Convers.*, 2008, **23**, (2), pp. 363–371
14 Teodorescu, R., Liserre, M., Rodriguez, P.: 'Grid converters for photovoltaic and wind power systems' (Wiley Press, 2011, 1st edn.)
15 Li, H., Chen, Z.: 'Overview of different wind generator systems and their comparisons', *IET Renew. Power Gener.*, 2008, **2**, (2), pp. 123–138
16 Engelhardt, S., Kretschmann, J., Fortmann, J., Shewarega, F., Feltes, C., Erlich, I.: 'Negative sequence control of DFG based wind turbines'. Proc. IEEE Power and Energy Society General Meeting, 2011, pp. 1–8
17 Conroy, J.F., Watson, R.: 'Low-voltage ride-through of a full converter wind turbine with permanent magnet generator', *IET Renew. Power Gener.*, 2007, **1**, (3), pp. 182–189
18 Conroy, J.F., Watson, R.: 'Aggregate modelling of wind farms containing full-converter wind turbine generators with permanent magnet synchronous machines: transient stability studies', *IET Renew. Power Gener.*, 2009, **3**, (1), pp. 39–52
19 Teodorescu, R., Blaabjerg, F., Liserre, M., Loh, P.C.: 'Proportional-resonant controllers and filters for grid-connected voltage-source converters', *Proc. IEE Electr. Power Appl.*, 2006, **153**, (5), pp. 750–762
20 Rodriguez, P., Luna, A., Candela, I., Mujal, R., Teodorescu, R., Blaabjerg, F.: 'Multiresonant frequency-locked loop for grid

synchronization of power converters under distorted grid conditions', *IEEE Trans. on Ind. Electr.*, 2011, **58**, (1), pp. 127–138
21 Rodriguez, P., Timbus, A., Teodorescu, R., Liserre, M., Blaabjerg, F.: 'Flexible active power control of distributed power generation systems during grid faults', *IEEE Trans. Ind. Electr.*, 2007, **54**, pp. 2583–2592
22 Saccomando, G., Svensson, J.: 'Transient operation of grid-connected voltage source converter under unbalanced voltage conditions'. Proc. IAS Annual Meeting, 2001, vol. 4, pp. 2419–2424
23 Sannino, A., Bollen, M.H. J., Svensson, J.: 'Voltage tolerance testing of three-phase voltage source converters', *IEEE Trans. Power Delivery*, 2005, **20**, (2), pp. 1633–1639
24 Alepuz, S., Busquets-Monge, S., Bordonau, J., *et al.*: 'Control strategies based on symmetrical components for grid-connected converters under voltage dips', *IEEE Trans. Ind. Electr.*, 2009, **56**, (6), pp. 2162–2173
25 Lee, C.-T., Hsu, C.-W., Cheng, P.-T.: 'A low-voltage ride-through technique for grid-connected converters of distributed energy resources', *IEEE Trans. Ind. Appl.*, 2011, **47**, (4), pp. 1821–1832
26 Castilla, M., Miret, J., Camacho, A., Matas, J., Alarcón-Gallo, E., de Vicuna, L.G.: 'Coordinated reactive power control for static synchronous compensators under unbalanced voltage sags'. IEEE Int. Symp. on Industrial Electronics (ISIE), 2012, pp. 987–992
27 Wang, F., Duarte, J.L., Hendrix, M.A.M.: 'Control of grid-interfacing inverters with integrated voltage unbalance correction'. IEEE Power Electronics Specialists Conf. (PESC), 2008, pp. 310–316
28 Camm, E.H., Behnke, M.R., Bolado, O., *et al.*: 'Wind power plant grounding, overvoltage protection, and insulation coordination: IEEE PES wind plant collector system design working group'. Proc. IEEE Power and Energy Society General Meeting, July 2009, pp. 1–8
29 Saadat, H.: 'Power system analysis' (McGraw-Hill Press, 1999, 2nd edn.)
30 Neumann, T., Feltes, C., Erlich, I.: 'Response of DFG-based wind farms operating on weak grids to voltage sags'. Proc. IEEE Power and Energy Society General Meeting, 2011, pp. 1–6
31 Cheng, Y., Sahni, M., Conto, J., Huang, S.-H., Schmall, J.: 'A voltage-profile based approach for developing collection system aggregated models for wind generation resources for grid VRT studies', *IET Renew. Power Gener.*, 2011, **5**, (5), pp. 332–346
32 Ottersten, R., Petersson, A., Pietiläinen, K.: 'Voltage sag response of PWM rectifiers for variable-speed wind turbines'. Nordic Workshop on Power and Industrial Electronics (NORpie), Trondheim, Norway, 2004
33 Mohseni, M., Islam, S., Masoum, M.A.S.: 'Impacts of symmetrical and asymmetrical voltage sags on DFIG-based wind turbines considering phase-angle jump, voltage recovery, and sag parameters', *IEEE Trans. Power Electr.*, 2011, **26**, (5), pp. 1587–1598

9 Appendix

See Table 3.

Table 3 Electrical data of lines and WPP components, S_{base} = 100 MVA, (pu)

		R	*X*	*B*
grid	Pos.	0.01	0.1	—
	Neg.	0.01	0.1	—
	Zero.	0.02	0.2	—
OHL	Pos.	0.022	0.112	0.026
	Neg.	0.022	0.112	0.026
	Zero.	0.088	0.372	0.014
equivalent collector network	Pos.	0.0056	0.0069	0.0175
	Neg.	0.0056	0.0069	0.0175
	Zero.	0.0589	0.0039	0.035
main Trf		0.01	0.15	—
WT Trf		0.008	0.08	—
ZZ Trf		0.01	0.1	—
WT filter		0.01	0.1	0.05
fault impedance		0.02	0	0

doi: 10.1049/iet-rpg.2012.0255